INTERNATIONAL JOURNAL FOR NUMERICAL METHODS IN FLUIDS
Int. J. Numer. Meth. Fluids 2005; **49**:267–299
Published online 23 May 2005 in Wiley InterScience (www.interscience.wiley.com). DOI: 10.1002/fld.992

Coupling between shallow water and solute flow equations: analysis and management of source terms in 2D

J. Murillo[‡], J. Burguete[§], P. Brufau[¶] and P. García-Navarro[*,†]

Fluid Dynamics, C.P.S. University of Zaragoza, Zaragoza, Spain

SUMMARY

A two-dimensional model for the simulation of solute transport by convection and diffusion into shallow water flow over variable bottom is presented. It is based on a finite volume method over triangular unstructured grids. A first order upwind technique is applied to solve the flux terms in both the flow and solute equations and the bed slope source terms and a centred discretization is applied to the diffusion and friction terms. The convenience of considering the fully coupled system of equations is indicated and the methodology is well explained. Three options are suggested and compared in order to deal with the diffusion terms. Some comparisons are carried out in order to show the performance in terms of accuracy and computational effort of the different options. Copyright © 2005 John Wiley & Sons, Ltd.

KEY WORDS: solute transport; convection; diffusion; shallow water flow; source terms; coupled system; finite volumes; two-dimensional model; conservation

1. INTRODUCTION

In the modelling of passive solute transport by shallow water flows, it is very common to solve the depth-averaged solute transport equation apart from the shallow water equations, that is, using a decoupled algorithm in which, first, the flow pattern is known and then the transport in that flow field is calculated [1, 2]. The reason for this is the physical assumption that, for low concentrations, the solute dynamics does not influence the flow behaviour, justifying then the use of a simpler decoupled resolution algorithm. It is also frequent to express and to use the solute transport equation in a non-conservative form, assuming that the velocities, depth, and the bottom level vary smoothly in time and space. Also, when the diffusion is not dominant, the transport problem can be considered as a linear advection problem in which the advection velocity is the flow velocity. The traditional numerical techniques applied to the

*Correspondence to: Pilar García-Navarro, Fluid Dynamics, C.P.S. University of Zaragoza, Zaragoza, Spain.
†E-mail: pigar@unizar.es
‡E-mail: jmurillo@mafalda.cps.unizar.es
§E-mail: jburguete@able.es
¶E-mail: brufau@unizar.es

Received 10 December 2004
Revised 7 April 2005
Accepted 11 April 2005

non-conservative form of the decoupled solute transport equation are of the semi-Lagrangian type and do not have, in general, the property of being conservative.

In many practical applications, however, when the properties of the flow change fast in time and/or in space, this approach can be inappropriate and lead to inaccurate solutions. The necessity to adopt a conservative formulation not only for the water flow but also for the solute flow equation arises, otherwise the numerical mass error generated may become important. The advection velocity in this case depends both on the solute concentration distribution and on the water depth. Some successful efforts have been devoted to ensure the conservation property in semi-Lagrangian schemes [3, 4] as applied to a single scalar equation. However, this work has been based on a fully conservative formulation on finite volumes applied to the coupled system governing both the water and solute motion that solves the system on triangular unstructured grids.

In this work, the coupling proves beneficial in avoiding numerical instabilities in the solute concentration when applied to complex situations. On the other hand, the coupling of the equations and the application of an upwind scheme generate numerical source terms both in the water and in the solute mass conservation equation. This leads to the necessity of a complete upwind treatment of the bed variation source terms that ensures the best balance in steady state cases. This has already been pointed out in many previous works in the context of shallow water flows [5, 6], but is even more obvious when extending the system of conservation laws to include the solute concentration equation.

Furthermore, the finite volume scheme used is explicit, which implies a restriction on the time step size that can be severe in presence of diffusion. Various techniques are presented and tested, where the time step is governed by a combination of the Peclet (Pe) and the Courant–Freidrichs–Lewy (CFL) numbers. Finally, a splitting technique is adopted to solve diffusion implicitly, avoiding small values of time step and allowing high accuracy, without increasing the numerical diffusion.

In order to evaluate the performance of the numerical transport model in unsteady complex situations for which there is not analytical solution, a two-dimensional laboratory dam break test case has been taken from the literature. Having calibrated the shallow flow model with the supplied water depth experimental data [5], this flow field is used as a basis for the solute transport test cases. First the pure advection problem is presented to highlight the importance of the conservative formulation in presence of discontinuous initial conditions. Then, different amounts of diffusion are assumed in order to evaluate, not only the influence of this term, but also the convenience of using the three different numerical strategies proposed to deal with it. On the other hand, the presence of a variable bottom level is also considered starting first by the basic requirement that the conservative method is able to keep constant an initial condition of still water. Then, the unsteady behaviour over variable bottom is analysed.

2. GOVERNING EQUATIONS

2.1. 2D mathematical model

The two-dimensional shallow water equations, which represent mass and momentum conservation in a plane, can be obtained by depth-averaging the Navier–Stokes equations. Neglecting diffusion of momentum due to viscosity and turbulence, wind effects and the Coriolis term,

they form the following system of equations [7]:

$$\frac{\partial \mathbf{U}_1}{\partial t} + \frac{\partial \mathbf{F}_1(\mathbf{U}_1)}{\partial x} + \frac{\partial \mathbf{G}_1(\mathbf{U}_1)}{\partial y} = \mathbf{S}_1(x, y, \mathbf{U}_1) \tag{1}$$

in which

$$\mathbf{U}_1 = (h, q_x, q_y)^{\mathrm{T}}$$

$$\mathbf{F}_1 = \left(q_x, \frac{q_x^2}{h} + \frac{gh^2}{2}, \frac{q_x q_y}{h}\right)^{\mathrm{T}}, \quad \mathbf{G}_1 = \left(q_y, \frac{q_x q_y}{h}, \frac{q_y^2}{h} + \frac{gh^2}{2}\right)^{\mathrm{T}}$$

where $q_x = uh$ and $q_y = vh$. The variable h represents the water depth, g is the acceleration of the gravity and (u, v) are the averaged components of the velocity vector $\mathbf{u}$ along the x and y coordinates, respectively. The source terms in the momentum equations are the contributions of bed slopes and the friction losses along the two coordinate directions,

$$\mathbf{S}_1 = (0, gh(S_{0x} - S_{fx}), gh(S_{0y} - S_{fy}))^{\mathrm{T}}$$

with the bed slopes in terms of the bottom level z,

$$S_{0x} = -\frac{\partial z}{\partial x}, \quad S_{0y} = -\frac{\partial z}{\partial y}$$

and the friction losses in terms of the Manning's roughness coefficient n [5]:

$$S_{fx} = \frac{n^2 u\sqrt{u^2 + v^2}}{h^{4/3}}, \quad S_{fy} = \frac{n^2 v\sqrt{u^2 + v^2}}{h^{4/3}}$$

In the context of a depth-averaged model, the depth-averaged concentration is of primary interest, and it has been shown that, under special conditions, an advection–dispersion model [8] can be defined as

$$\frac{\partial (h\phi)}{\partial t} + \vec{\nabla}(\mathbf{u}h\phi) = \vec{\nabla}(\mathbf{K}h\vec{\nabla}\phi) \tag{2}$$

where ϕ is the depth-averaged concentration, and $\mathbf{K}$ is an empirical dispersion matrix that should not be confused with the turbulent diffusivity. In general, $\mathbf{K}$ incorporates dispersion due to differential advection as well as turbulent diffusion [9].

Traditionally, both models (1) and (2) have been solved independently in a sequential form, solving first the shallow water equations and next, in function of those flow values, the solute flow equation. In order to improve the accuracy and conservation properties of the solution, both models are coupled in a single system of equations, that becomes

$$\frac{\partial \mathbf{U}}{\partial t} + \frac{\partial \mathbf{F}(\mathbf{U})}{\partial x} + \frac{\partial \mathbf{G}(\mathbf{U})}{\partial y} = \mathbf{S}(x, y, \mathbf{U}) \tag{3}$$

where

$$\mathbf{U} = (h, q_x, q_y, h\phi)^{\mathrm{T}} = (h, q_x, q_y, m)^{\mathrm{T}}$$

$$\mathbf{F} = \left(q_x, \frac{q_x^2}{h} + \frac{gh^2}{2}, \frac{q_x q_y}{h}, mu\right)^{\mathrm{T}}, \quad \mathbf{G} = \left(q_y, \frac{q_x q_y}{h}, \frac{q_y^2}{h} + \frac{gh^2}{2}, mv\right)^{\mathrm{T}}$$

$$\mathbf{S} = (0, gh(S_{0x} - S_{fx}), gh(S_{0y} - S_{fy}), \vec{\nabla}(\mathbf{K}h\vec{\nabla}\phi))^{\mathrm{T}}$$

The source term vector is split in three different parts treated separately: bottom variations **B**, diffusion term **D**, and friction term **R**: $\mathbf{S} = \mathbf{B} + \mathbf{D} + \mathbf{R}$

$$\mathbf{B} = (0, ghS_{0x}, ghS_{0y}, 0)^{\mathrm{T}}$$

$$\mathbf{D} = (0, 0, 0, \vec{\nabla}(\mathbf{K}h\vec{\nabla}\phi))^{\mathrm{T}}$$

$$\mathbf{R} = (0, -ghS_{fx}, -ghS_{fy}, 0)^{\mathrm{T}}$$

It is useful to rewrite (3) as

$$\frac{\partial \mathbf{U}}{\partial t} + \vec{\nabla}\mathbf{E}(\mathbf{U}) = \mathbf{S}(x, y, \mathbf{U}) \tag{4}$$

in which the flux $\mathbf{E} = (\mathbf{F}, \mathbf{G})^{\mathrm{T}}$ is linked to the conservative character of the system in the absence of source terms, and in order to introduce the integral form of the equation over a fixed volume Ω,

$$\frac{\partial}{\partial t}\int_{\Omega} \mathbf{U}\,\mathrm{d}\Omega + \int_{\Omega} (\vec{\nabla}\mathbf{E})\,\mathrm{d}\Omega = \int_{\Omega} \mathbf{S}\,\mathrm{d}\Omega \tag{5}$$

Gauss's theorem applied to the flux integral gives

$$\frac{\partial}{\partial t}\int_{\Omega} \mathbf{U}\,\mathrm{d}\Omega + \oint_{\partial\Omega} (\mathbf{E}\cdot\mathbf{n})\,\mathrm{d}s = \int_{\Omega} \mathbf{S}\,\mathrm{d}\Omega \tag{6}$$

where $\partial\Omega$ denotes the surface surrounding the volume Ω and **n** is the unit outward normal vector to the cell.

3. NUMERICAL METHOD

A cell-centred finite volume method is formulated where all the dependent variables of the system are represented as piecewise constants (first order). In the two-dimensional approach presented in this work, the spatial domain of integration is covered by a set of triangular cells, not aligned with the two coordinate directions. A discrete approximation of Equation (6)

is applied in every cell Ω_i at a given time so that the volume integrals represent integrals over the area of the cell and the surface integrals represent the total flux through the cell boundaries. Denoting by $\mathbf{U}_i$ the average value of the conservative variables over the volume Ω_i at a given time, from Equation (6) the following conservation equation can be written for every cell:

$$\frac{\partial \mathbf{U}_i}{\partial t} A_i + \oint_{\partial\Omega} (\mathbf{E} \cdot \mathbf{n})\, \mathrm{d}s = \int_{\Omega} \mathbf{S}\, \mathrm{d}\Omega \tag{7}$$

where A_i is the area of the cell Ω_i.

A mesh fixed in time is assumed and the contour integral is approached by a sum over the cell edges. In all of them, the normal flux is evaluated via an upwind flux difference splitting technique

$$\oint_{\partial\Omega_i} (\mathbf{E} \cdot \mathbf{n})\, \mathrm{d}s \approx \sum_{k=1}^{\mathrm{NE}} (\delta \mathbf{E}_k \cdot \mathbf{n}_k) s_k \tag{8}$$

where k represents the edges index of the cell Ω_i, NE is the total number of edges in the cell (NE = 3). The vector $\mathbf{n}_k$ is the unit outward normal to edge k, s_k is the length of the side, and $\delta \mathbf{E}_k \cdot \mathbf{n}_k$ is the numerical flux difference. Upwind schemes are based on the idea of discretizing the spatial derivates so that the information is taken from the side it comes. When the source terms are present, it has previously been shown that the flux derivates and the source terms have to be discretized in a similar manner [5, 10]. The evaluation of fluxes and sources at the same local state is important.

The mathematical properties of the hyperbolic system we are dealing with include the existence of a Jacobian matrix, $\mathbf{J}_\mathbf{n}$, of the normal flux $(\mathbf{E} \cdot \mathbf{n})$ defined as

$$\mathbf{J}_\mathbf{n} = \frac{\partial (\mathbf{E} \cdot \mathbf{n})}{\partial \mathbf{U}} = \frac{\partial (\mathbf{F})}{\partial \mathbf{U}} n_x + \frac{\partial (\mathbf{G})}{\partial \mathbf{U}} n_y$$

that can be expressed in terms of the conserved variables as

$$\mathbf{J}_\mathbf{n} = \begin{pmatrix} 0 & n_x & n_y & 0 \\ \left(gh - \dfrac{q_x^2}{h^2}\right) n_x - \dfrac{q_x q_y}{h^2} n_y & \dfrac{q_y}{h} n_y + \dfrac{2q_x}{h} n_x & \dfrac{q_x}{h} n_y & 0 \\ \left(gh - \dfrac{q_y^2}{h^2}\right) n_y - \dfrac{q_x q_y}{h^2} n_x & \dfrac{q_y}{h} n_x & \dfrac{q_x}{h} n_x + \dfrac{2q_y}{h} n_y & 0 \\ -\left(\dfrac{q_x}{h^2} n_x + \dfrac{q_y}{h^2} n_y\right) m & \dfrac{m}{h} n_x & \dfrac{m}{h} n_y & \left(\dfrac{q_x}{h} n_x + \dfrac{q_y}{h} n_y\right) \end{pmatrix}$$

The eigenvalues of $\mathbf{J_n}$ are a representation of the characteristic speeds

$$\begin{aligned}\lambda^1 &= \mathbf{u}\cdot\mathbf{n} + c\\ \lambda^2 &= \mathbf{u}\cdot\mathbf{n}\\ \lambda^3 &= \mathbf{u}\cdot\mathbf{n} - c\\ \lambda^4 &= \mathbf{u}\cdot\mathbf{n}\end{aligned} \tag{9}$$

where $\mathbf{u}=(u,v)$, $\mathbf{n}=(n_x,n_y)$ and $c=\sqrt{gh}$ is the celerity of small amplitude surface waves. The corresponding right eigenvectors are

$$\mathbf{e}^1=\begin{pmatrix}1\\ u+cn_x\\ v+cn_y\\ \phi\end{pmatrix},\quad \mathbf{e}^2=\begin{pmatrix}0\\ -cn_y\\ cn_x\\ 2\phi\end{pmatrix},\quad \mathbf{e}^3=\begin{pmatrix}1\\ u-cn_x\\ v-cn_y\\ \phi\end{pmatrix},\quad \mathbf{e}^4=\begin{pmatrix}0\\ 0\\ 0\\ 1\end{pmatrix} \tag{10}$$

From its eigenvectors, two matrices $\mathbf{P}$ and $\mathbf{P}^{-1}$ can be constructed with the property that they diagonalize the Jacobian $\mathbf{J_n}$.

$$\mathbf{J_n}=\mathbf{P}\boldsymbol{\Lambda}\mathbf{P}^{-1}$$

where $\boldsymbol{\Lambda}$ is a diagonal matrix with eigenvalues in the main diagonal. Those matrices are

$$\begin{aligned}\mathbf{P} &= \begin{pmatrix}1 & 0 & 1 & 0\\ u+cn_x & -cn_y & u-cn_x & 0\\ v+cn_y & cn_x & v-cn_y & 0\\ \phi & 2\phi & \phi & 1\end{pmatrix},\\ \mathbf{P}^{-1} &= \frac{1}{2c}\begin{pmatrix}-\mathbf{u}\cdot\mathbf{n}+c & n_x & n_y & 0\\ 2(un_y-vn_x) & -2n_y & 2n_x & 0\\ \mathbf{u}\cdot\mathbf{n}+c & -n_x & -n_y & 0\\ -2\phi(c+2(un_y-vn_x)) & 4\phi n_y & -4\phi n_x & 1\end{pmatrix}\end{aligned} \tag{11}$$

The existence of the Jacobian matrix and the differential relation among conserved variables, fluxes and Jacobian allows a local linearization in the form

$$\delta(\mathbf{E}\cdot\mathbf{n})=\tilde{\mathbf{J}}_{RL}\delta\mathbf{U}$$

that can be used for the discretization of the normal flux difference across the edge between the computational cells Ω_L on the left and Ω_R on the right (normal vector at the edge pointing from L to R). This requires the definition of an approximated flux Jacobian, $\tilde{\mathbf{J}}_{RL}$, constructed at the edges of the cells, taking into account the information provided by the right cell Ω_R

and the left cell Ω_L. Note that subscript k is omitted. As suggested by Roe [11] the matrix $\tilde{\mathbf{J}}_{RL}$ has the same form as $\mathbf{J_n}$ but is evaluated at an average state defined by the quantities $\tilde{\mathbf{u}} = (\tilde{u}, \tilde{v})$, $\tilde{c}$ and $\tilde{\phi}$, which must be calculated according to a set of the matrix properties:

(1) $\tilde{\mathbf{J}}_{RL} = \tilde{\mathbf{J}}_{RL}(\mathbf{U}_R, \mathbf{U}_L)$.
(2) $(\mathbf{E}\cdot\mathbf{n})_R - (\mathbf{E}\cdot\mathbf{n})_L = \tilde{\mathbf{J}}_{RL}(\mathbf{U}_R - \mathbf{U}_L)$.
(3) $\tilde{\mathbf{J}}_{RL}$ has real eigenvalues and a set of eigenvectors.
(4) $\tilde{\mathbf{J}}_{RL} = \tilde{\mathbf{J}}_{RL}(\mathbf{U}_L) = \tilde{\mathbf{J}}_{RL}(\mathbf{U}_R)$ if $\mathbf{U}_L = \mathbf{U}_R$.

In order to identify the intermediate states of the four involved variables, a new set of matrices must be created [12]:

$$\mathbf{Z} = \frac{1}{\sqrt{h}}\mathbf{U} = (z_1, z_2, z_3, z_4)^{\mathrm{T}}, \quad \tilde{\mathbf{Z}} = \frac{1}{2}(\mathbf{Z}_R + \mathbf{Z}_L) \tag{12}$$

and the following change of variable is defined:

$$\delta\mathbf{U} = \mathbf{E}\cdot\delta\mathbf{Z} \tag{13}$$

where

$$\mathbf{E} = \begin{pmatrix} 2\tilde{z}_1 & 0 & 0 & 0 \\ \tilde{z}_2 & \tilde{z}_1 & 0 & 0 \\ \tilde{z}_3 & 0 & \tilde{z}_1 & 0 \\ \tilde{z}_4 & 0 & 0 & \tilde{z}_1 \end{pmatrix}, \quad \mathbf{E}^{-1} = \begin{pmatrix} (2\tilde{z}_1^2)^{-1} & 0 & 0 & 0 \\ -\tilde{z}_2(2\tilde{z}_1^2)^{-1} & \tilde{z}_1^{-1} & 0 & 0 \\ -\tilde{z}_3(2\tilde{z}_1^2)^{-1} & 0 & \tilde{z}_1^{-1} & 0 \\ -\tilde{z}_4(2\tilde{z}_1^2)^{-1} & 0 & 0 & \tilde{z}_1^{-1} \end{pmatrix}$$

It can also be seen that

$$\delta\mathbf{F} = \mathbf{C}_1\cdot\delta\mathbf{Z}, \quad \delta\mathbf{G} = \mathbf{C}_2\cdot\delta\mathbf{Z} \tag{14}$$

with

$$\mathbf{C}_1 = \begin{pmatrix} \tilde{z}_2 & \tilde{z}_1 & 0 & 0 \\ 2c^2\tilde{z}_1 & 2\tilde{z}_2 & 0 & 0 \\ 0 & \tilde{z}_3 & \tilde{z}_2 & 0 \\ 0 & \tilde{z}_4 & 0 & \tilde{z}_2 \end{pmatrix}, \quad \mathbf{C}_2 = \begin{pmatrix} \tilde{z}_3 & 0 & \tilde{z}_1 & 0 \\ 0 & \tilde{z}_3 & \tilde{z}_2 & 0 \\ 2c^2\tilde{z}_1 & 0 & 2\tilde{z}_3 & 0 \\ 0 & 0 & \tilde{z}_4 & \tilde{z}_3 \end{pmatrix}$$

With the help of these matrices the following can be written:

$$\delta\mathbf{F}n_x + \delta\mathbf{G}n_y = (\mathbf{C}_1 n_x + \mathbf{C}_2 n_y)\delta\mathbf{Z} = (\mathbf{C}_1 n_x + \mathbf{C}_2 n_y)\mathbf{E}^{-1}\delta\mathbf{U} = \tilde{\mathbf{J}}_{RL}\cdot\delta\mathbf{U} \tag{15}$$

so that

$$\tilde{\mathbf{J}}_{RL} = \begin{pmatrix} 0 & n_x & n_y & 0 \\ \tilde{c}^2 n_x - \tilde{\mathbf{u}}\cdot\mathbf{n}\tilde{u} & \tilde{u}n_x + \tilde{\mathbf{u}}\cdot\mathbf{n} & \tilde{u}n_y & 0 \\ \tilde{c}^2 n_y - \tilde{\mathbf{u}}\cdot\mathbf{n}\tilde{v} & \tilde{v}n_x & \tilde{v}n_y + \tilde{\mathbf{u}}\cdot\mathbf{n} & 0 \\ -\tilde{\mathbf{u}}\cdot\mathbf{n}\tilde{\phi} & \tilde{\phi}n_x & \tilde{\phi}n_y & \tilde{\mathbf{u}}\cdot\mathbf{n} \end{pmatrix} \tag{16}$$

with

$$\tilde{u} = \frac{u_R\sqrt{h_R} + u_L\sqrt{h_L}}{\sqrt{h_R} + \sqrt{h_L}}, \quad \tilde{v} = \frac{v_R\sqrt{h_R} + v_L\sqrt{h_L}}{\sqrt{h_R} + \sqrt{h_L}}$$
$$\tilde{c} = \sqrt{g\frac{(h_R + h_L)}{2}}, \quad \tilde{\phi} = \frac{\phi_R\sqrt{h_R} + \phi_L\sqrt{h_L}}{\sqrt{h_R} + \sqrt{h_L}} \tag{17}$$

The eigenvalues of $\tilde{\mathbf{J}}_{RL}$ are

$$\begin{aligned} \tilde{\lambda}^1 &= \tilde{\mathbf{u}} \cdot \mathbf{n} + \tilde{c} \\ \tilde{\lambda}^2 &= \tilde{\mathbf{u}} \cdot \mathbf{n} \\ \tilde{\lambda}^3 &= \tilde{\mathbf{u}} \cdot \mathbf{n} - \tilde{c} \\ \tilde{\lambda}^4 &= \tilde{\mathbf{u}} \cdot \mathbf{n} \end{aligned} \tag{18}$$

and the corresponding eigenvectors

$$\tilde{\mathbf{e}}^1 = \begin{pmatrix} 1 \\ \tilde{u} + \tilde{c}n_x \\ \tilde{v} + \tilde{c}n_y \\ \tilde{\phi} \end{pmatrix}, \quad \tilde{\mathbf{e}}^2 = \begin{pmatrix} 0 \\ -\tilde{c}n_y \\ \tilde{c}n_x \\ 2\tilde{\phi} \end{pmatrix}, \quad \tilde{\mathbf{e}}^3 = \begin{pmatrix} 1 \\ \tilde{u} - \tilde{c}n_x \\ \tilde{v} - \tilde{c}n_y \\ \tilde{\phi} \end{pmatrix}, \quad \tilde{\mathbf{e}}^4 = \begin{pmatrix} 0 \\ 0 \\ 0 \\ 1 \end{pmatrix} \tag{19}$$

Following the basic flux difference procedure, the difference in vector $\mathbf{U}$ across the grid edge is projected onto the matrix eigenvectors basis as

$$\delta\mathbf{U} = \mathbf{U}_R - \mathbf{U}_L = \sum_{m=1}^{4} \alpha^m \tilde{\mathbf{e}}^m \tag{20}$$

where the expressions of coefficients α^m are

$$\begin{aligned} \alpha^{1,3} &= \frac{h_R - h_L}{2} \pm \frac{1}{2\tilde{c}}[((hu)_R - (hu)_L)n_x + ((hv)_R - (hv)_L)n_y - (\tilde{u}n_x + \tilde{v}n_y)(h_R - h_L)] \\ \alpha^2 &= \frac{1}{\tilde{c}}[[((hv)_R - (hv)_L) - \tilde{v}(h_R - h_L)]n_x - [((hu)_R - (hu)_L) - \tilde{u}(h_R - h_L)]n_y] \\ \alpha^4 &= ((h\phi)_R - (h\phi)_L) - \tilde{\phi}(h_R - h_L + 2\alpha^2) \end{aligned} \tag{21}$$

Therefore, the matrix $\tilde{\mathbf{J}}_{RL}$ is replaced by its eigenvalues and eigenvectors in the product $\tilde{\mathbf{J}}_{RL}(\mathbf{U}_R - \mathbf{U}_L)$ in the form

$$\tilde{\mathbf{J}}_{RL}(\mathbf{U}_R - \mathbf{U}_L) = \sum_{m=1}^{4} \tilde{\lambda}^m \alpha^m \tilde{\mathbf{e}}^m \tag{22}$$

In order to discriminate the sense of advection linked to the different eigenvalues two matrices $\mathbf{\Lambda}^{\pm}$ are defined, where $\mathbf{\Lambda}^{\pm} = (\mathbf{\Lambda} \pm |\mathbf{\Lambda}|)/2$ so that

$$\begin{aligned} \delta(\mathbf{E}\cdot\mathbf{n}) &= \tilde{\mathbf{J}}_{RL}\delta\mathbf{U} = \tilde{\mathbf{P}}\tilde{\mathbf{\Lambda}}\tilde{\mathbf{P}}^{-1}\delta\mathbf{U} = \tilde{\mathbf{P}}(\tilde{\mathbf{\Lambda}}^{+} + \tilde{\mathbf{\Lambda}}^{-})\tilde{\mathbf{P}}^{-1}\delta\mathbf{U} \\ \delta(\mathbf{E}\cdot\mathbf{n}) &= \underbrace{\tilde{\mathbf{P}}\tilde{\mathbf{\Lambda}}^{-}\tilde{\mathbf{P}}^{-1}\delta\mathbf{U}}_{\text{in-going waves}} + \underbrace{\tilde{\mathbf{P}}\tilde{\mathbf{\Lambda}}^{+}\tilde{\mathbf{P}}^{-1}\delta\mathbf{U}}_{\text{out-going waves}} \end{aligned} \tag{23}$$

For the updating, only the in-going contributions generated at the edges surrounding a cell are of interest so that the contour integral of the numerical normal flux is equivalent to the sum of the in-going waves. The cell variation of $\mathbf{U}$, neglecting the source terms, can be defined as

$$\frac{\partial \mathbf{U}_i}{\partial t} A_i = -\sum_{k=1}^{\mathrm{NE}} \sum_{m=1}^{4} (\tilde{\lambda}^{m-} \alpha^m \tilde{\mathbf{e}}^m)_i^n s_k \tag{24}$$

where it has been used that

$$\tilde{\mathbf{P}}\tilde{\mathbf{\Lambda}}^{-}\tilde{\mathbf{P}}^{-1}\delta\mathbf{U} = \sum_{m=1}^{4} \tilde{\lambda}^{m-} \alpha^m \tilde{\mathbf{e}}^m \tag{25}$$

and $\lambda^{-} = (\lambda - |\lambda|)/2$.

3.1. Bottom variations

Given the derivative form of the bed slope source terms, an upwind approach has been adopted to model them in order to ensure the best balance with the flux terms at least in steady state cases. For every cell edge k of cell Ω_i the discrete source term is decomposed into inward and outward contributions as before

$$\mathbf{B}_k = \mathbf{B}_k^{+} + \mathbf{B}_k^{-}$$

being

$$\mathbf{B}_k^{\pm} = \tilde{\mathbf{P}}(\mathbf{I} \pm |\tilde{\mathbf{\Lambda}}|\tilde{\mathbf{\Lambda}}^{-})\tilde{\mathbf{P}}^{-1}\mathbf{B}_{RL} = \sum_{m=1}^{4} \beta^{m\pm} \tilde{\mathbf{e}}^m \tag{26}$$

The average value $\mathbf{B}_{RL}$ is computed with

$$\mathbf{B}_{RL} = \begin{pmatrix} 0 \\ g\dfrac{h_L + h_R}{2}\delta z_x \\ g\dfrac{h_L + h_R}{2}\delta z_y \\ 0 \end{pmatrix}_k = \begin{pmatrix} 0 \\ S_2 \\ S_3 \\ 0 \end{pmatrix}_k \tag{27}$$

where the bed increments in each direction are

$$\delta z_x = -(z_R - z_L)n_x, \quad \delta z_y = -(z_R - z_L)n_y \tag{28}$$

The expressions for the β^- coefficients are

$$\begin{aligned}
\beta^{1-} &= \frac{1}{2\tilde{c}}(S_2 n_x + S_3 n_y)(1 - \mathrm{sgn}(\tilde{\lambda}_1)) \\
\beta^{2-} &= \frac{1}{\tilde{c}}(-S_2 n_y + S_3 n_x)(1 - \mathrm{sgn}(\tilde{\lambda}_2)) \\
\beta^{3-} &= \frac{-1}{2\tilde{c}}(S_2 n_x + S_3 n_y)(1 - \mathrm{sgn}(\tilde{\lambda}_3)) \\
\beta^{4-} &= \frac{-1}{\tilde{c}} 2\tilde{\phi}(S_2 n_y - S_3 n_x)(1 - \mathrm{sgn}(\tilde{\lambda}_4))
\end{aligned} \tag{29}$$

and, extending (24), the following partial updating rule is obtained for every cell:

$$\mathbf{U}_i^* = \mathbf{U}_i^n - \sum_{k=1}^{\mathrm{NE}} \sum_{m=1}^{4} ((\tilde{\lambda}^{m-}\alpha^m - \beta^{m-})\tilde{\mathbf{e}}^m)_i^n \frac{s_k}{A_i} \Delta t \tag{30}$$

The total contribution of the source term is made of the sum of the parts associated to inward normal velocity at every edge k. Note that the superscript $*$ indicates predictor value.

The time step size in explicit schemes like (30) is limited for numerical stability reasons and controlled by the Courant–Friedrichs–Lewy, *CFL* [5], dimensionless number

$$\begin{aligned}
\Delta t &= CFL \Delta t_{\max}^{CFL} \\
CFL &\leqslant 1
\end{aligned} \tag{31}$$

with

$$\begin{aligned}
\Delta t_{\max}^{CFL} &= \min\{\Delta t_{\max,i}^{CFL}\}_{i=1,\mathrm{NCELL}} \\
\Delta t_{\max,i}^{CFL} &= \left\{ \min\left(\frac{\min\{A_R, A_L\}}{\tilde{\lambda}_k^{m-}\, \mathrm{d}s_k} \right) \right\}_{k=1,\mathrm{NE}}
\end{aligned} \tag{32}$$

3.2. Solute flow diffusion

The integral of the diffusion term **D** is modified applying again Gauss's theorem,

$$\int_\Omega \vec{\nabla}(\mathbf{K} h \vec{\nabla}\phi)\, \mathrm{d}\Omega = \oint_{\partial\Omega} (\mathbf{K} h \vec{\nabla}\phi)\mathbf{n}\, \mathrm{d}s \tag{33}$$

The contour integral is approached by a sum over the cell edges:

$$\mathbf{D}_i = \int_{\Omega_i} \vec{\nabla}(\mathbf{K} h \vec{\nabla}\phi)\, \mathrm{d}\Omega = \oint_{\partial\Omega_i} (\mathbf{K} h \vec{\nabla}\phi)\mathbf{n}\, \mathrm{d}s = \sum_{k=1}^{\mathrm{NE}} (\mathbf{K} h \vec{\nabla}\phi)_k \mathbf{n}_k s_k \tag{34}$$

where $(\mathbf{K} h \vec{\nabla}\phi)_k$ can be discretized as

$$(\mathbf{K} h \vec{\nabla}\phi)_k = \frac{\mathbf{K}_R + \mathbf{K}_L}{2}\, \mathbf{n}\, \min(h_R^*, h_L^*)\, \frac{(\phi_R - \phi_L)}{d} \tag{35}$$

where d is the distance between the centers of cells R and L. Note that h is evaluated as $\min(h_R^*, h_L^*)$ in order to avoid diffusion in dry/wet edges. Depending on how $\delta\phi = (\phi_R - \phi_L)$

is evaluated and also on how the time step is chosen, various methods can be achieved. This is discussed next.

3.2.1. Technique (a) Explicit scheme. $\delta\phi$ is computed as $\delta\phi^n$,

$$\mathbf{U}_i^{n+1} = \mathbf{U}_i^n - \sum_{k=1}^{\mathrm{NE}} \sum_{m=4}^{3} ((\tilde{\lambda}^{m-} \alpha^m - \beta^{m-}) \tilde{\mathbf{e}}^m)_i^n \frac{s_k}{A_i} \Delta t + \int_\Omega \mathbf{D}_i^n \, \mathrm{d}\Omega \frac{\Delta t}{A_i} \tag{36}$$

The stability in this case is determined by the combination of diffusion and advection. The time step is limited by both the Peclet number, *Pe*, and the *CFL* number [13], so that

$$Pe + CFL \leqslant 1 \tag{37}$$

where $Pe = \frac{1}{2} \frac{\mathbf{K} \cdot \mathbf{n} \Delta t_{Pe}}{\delta x^2}$, $\quad \delta x = \min \left\{ \frac{A_i}{s_k} \right\}_{i=1,\mathrm{NCELL}, k=1,\mathrm{NE}}$

This scheme is linked to the most restrictive time step. When only diffusion is considered the time step is limited by $Pe \leqslant 1$.

3.2.2. Technique (b) Splitting technique and explicit diffusion. If a splitting technique is adopted, as suggested by Karpik and Crockett [14] first, the advection step is solved by means of (30), and a new value of ϕ^* in each cell is obtained. Then the diffusion is solved.

As the diffusion is computed separately, if this is made explicitly, the time step of the second step is limited by the *Pe* number. To avoid decreasing the value of the global time step, the following scheme is proposed. It essentially consists of accumulating diffusion steps until the global time step given by the CFL condition is reached:

$$\mathbf{U}_i^1 = \mathbf{U}_i^* + \int_\Omega \mathbf{D}_i^* \, \mathrm{d}\Omega \frac{\Delta t_{Pe}}{A_i}, \quad \mathbf{D}_i^* = \mathbf{D}(\mathbf{U}_i^*)$$

$$\vdots$$

$$\mathbf{U}_i^j = \mathbf{U}_i^{j-1} + \int_\Omega \mathbf{D}_i^{j-1} \, \mathrm{d}\Omega \frac{\Delta t_{Pe}}{A_i}, \quad \mathbf{D}_i^{j-1} = \mathbf{D}(\mathbf{U}_i^{j-1})$$

for $j = 1, \ldots, NT$ where $NT = \mathrm{int}[\Delta t / \Delta t_{Pe}]$, and finally,

$$\mathbf{U}_i^{n+1} = \mathbf{U}_i^{NT} + \int_\Omega \mathbf{D}_i^{NT} \, \mathrm{d}\Omega \frac{(\Delta t - NT \Delta t_{Pe})}{A_i} \tag{38}$$

3.2.3. Technique (c) Splitting technique and implicit diffusion. In this version of the splitting technique, after solving the advection step by means of (30) and obtaining a new value of ϕ^* in each cell, the value of ϕ^{n+1} is computed discretizing the diffusion in an implicit way as:

$$\mathbf{U}_i^{n+1} = \mathbf{U}_i^* + \int_\Omega \mathbf{D}^{n+1} \, \mathrm{d}\Omega \frac{\Delta t}{A_i} \tag{39}$$

The numerical model becomes unconditionally stable, as the resolution matrix is positive defined, so finally the time step used depends only on the value of *CFL* as if only advection was involved.

3.3. Friction terms

The friction term $\mathbf{R}$ is discretized in a pointwise manner $\mathbf{R}_i = \mathbf{R}_i^n$, so the final updating step consists of adding a friction term to the previously updated variable.

$$\mathbf{U}_i^{n+1} = \mathbf{U}_i^{n+1} + \int_\Omega \mathbf{R}\, \mathrm{d}\Omega\, \frac{\Delta t}{A_i} = \mathbf{U}_i^{n+1} + \mathbf{R}_i^n \Delta t \tag{40}$$

4. PROPERTIES OF THE PROPOSED SCHEME

One advantage of considering the shallow water equations and the solute flow equation as a coupled set of equations is that the conservative character of the numerical method is preserved in a simple way. When the solute flow is considered as a decoupled equation and discretized separately, the upwind technique leads to numerical difficulties. If an upwind finite volume approximation is applied to Equation (2), neglecting diffusion, the following must be written:

$$(h\phi)^{n+1} = (h\phi)^n + \sum_{k=1}^{\mathrm{NE}} (\tilde{\mathbf{u}}^\phi \cdot \mathbf{n})_k^- \delta\phi_k \frac{s_k}{A_i} \Delta t \tag{41}$$

where again $\delta\phi_k = \phi_R - \phi_L$, and, for conservation, in this case the following discrete advection velocity results

$$\tilde{\mathbf{u}}_k^\phi = \frac{1}{2}\left[\frac{\sqrt{h\phi}_R \mathbf{u}_R + \sqrt{h\phi}_L \mathbf{u}_L}{\sqrt{h\phi}_R + \sqrt{h\phi}_L} - \frac{\sqrt{h\phi}_R \mathbf{u}_R - \sqrt{h\phi}_L \mathbf{u}_L}{\sqrt{h\phi}_R - \sqrt{h\phi}_L} \right] \tag{42}$$

which reduces to $\tilde{\mathbf{u}}_k^\phi = \mathbf{u}$ only in trivial uniform flow situations. It is obvious, first, that the presence of a difference in the denominator of the second term can lead to numerical troubles when $\sqrt{h\phi}_R \approx \sqrt{h\phi}_L$. On the other hand, this average advection velocity is useless in cases of discontinuous water levels and zero water velocities despite the mass transfer predicted by the water flow equations. For instance, let us suppose one-dimensional dam break initial conditions, over a flat bed,

$$h(x,0) = \begin{cases} h_L & \text{if } x \leqslant x_0 \\ h_R & \text{if } x \geqslant x_0 \end{cases}, \quad u(x,0) = 0, \quad \phi(x,0) = \phi_0$$

with $h_L > h_R$. In this case, the rule proposed in (41) as applied to the interface located at the dam position (x_0) leads to

$$(h\phi)_L^{n+1} = (h\phi)_L^n, \quad (h\phi)_R^{n+1} = (h\phi)_R^n$$

and from (30) as applied to the water mass equation

$$h_L^{n+1} = h_L^n - \Delta h, \quad h_R^{n+1} = h_R^n + \Delta h$$

where $\Delta h = h_L - h_R > 0$. The final solute concentration at cells L and R is $\phi_L^{n+1} > \phi_0$ and $\phi_R^{n+1} < \phi_0$, respectively, so an incoherent result is obtained.

Instead, if the rule presented in (30) is applied it is simple to check that

$$h_L^{n+1} = h_L^n - \Delta h, \quad h_R^{n+1} = h_R^n + \Delta h$$

$$(h\phi)_L^{n+1} = (h\phi)_L^n - \Delta h\tilde{\phi}, \quad (h\phi)_R^{n+1} = (h\phi)_R^n + \Delta h\tilde{\phi}$$

where $\tilde{\phi} = \phi_0$, which can be rearranged to

$$(h\phi)_L^{n+1} = (h - \Delta h)\phi_0, \quad (h\phi)_R^{n+1} = (h + \Delta h)\phi_0$$

leading to $\phi_L^{n+1} = \phi_0$ and $\phi_R^{n+1} = \phi_0$, the correct final state.

5. APPLICATIONS

5.1. Asymmetric dam break with flat bed

The coupled model (30) and the decoupled model (42), where the solute flow equation is treated independently, are going to be compared by means of a test case of solute transport in a two-dimensional dam break simulation. The dam break set-up corresponds to an earlier laboratory experiment designed and performed by a team at the University of A Coruña (Spain) CITEEC in which a closed pool is divided in two parts by a section (Figure 1) where a gate (dam) is suddenly open giving rise to a wave pattern far from the one-dimensional

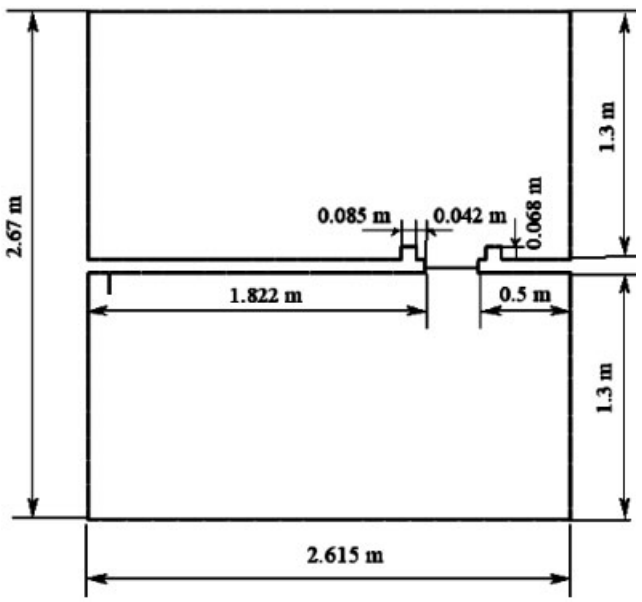

Figure 1. Coruña's laboratory set-up plan view.

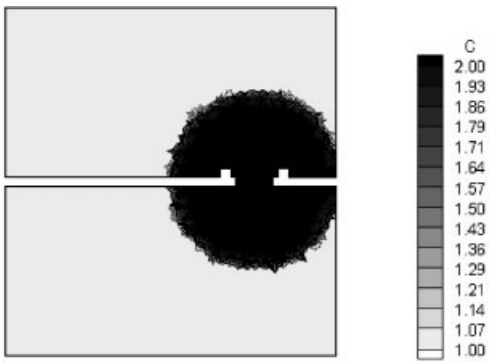

Figure 2. Initial concentration level.

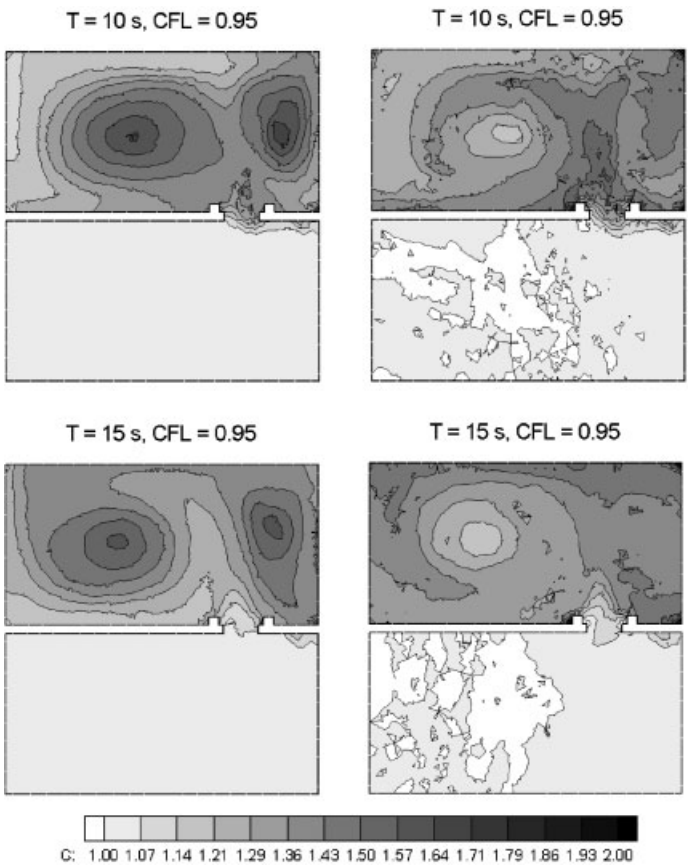

Figure 3. Isolines of concentration at times $t = 5, 10, 15$ s, with a coupled system (left), and decoupled resolution (right) of the pure advection problem.

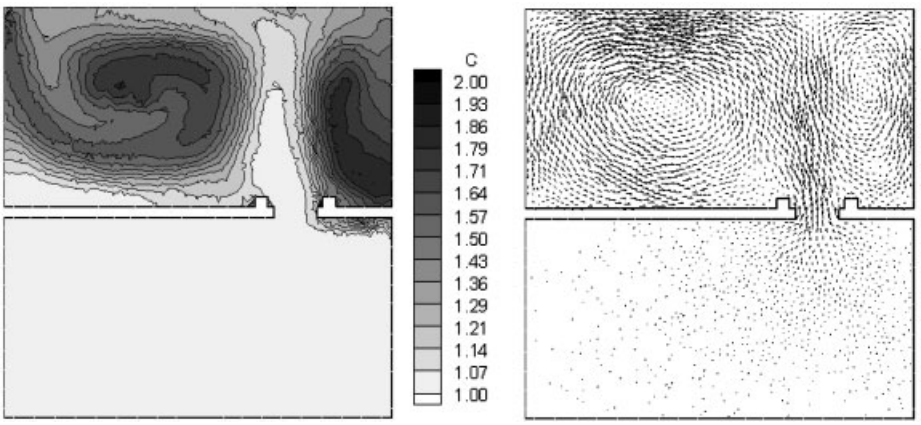

Figure 4. Isolines of concentration (left), and velocity vectors (right) at time $t = 5\,\mathrm{s}$ with coupled system. Pure advection.

distribution. The bed is horizontal and the experiment was performed for an initial depth ratio of 0.5/0.1 m [15]. An initial distribution of solute, not present in the experiment, has been assumed in this example. The initial concentration is a circular step distribution around the gate so that there is a jump, shown in Figure 2, and defined as

$$\phi(x, y, t_0 = 0) = \begin{cases} 2 & \text{if } r \leqslant r_0 \\ 1 & \text{if } r \geqslant r_0 \end{cases} \quad \text{with } r = ((x - 1.97)^2 + (x - 1.35)^2)^{1/2},\ r_0 = 0.65\,\mathrm{m}$$

The Manning's roughness parameter n used is 0.01 according to the tank's material. The computing mesh contains 7875 cells. In order to evaluate the differences between both coupled and decoupled advection models, the value of the dispersion coefficient $\mathbf{K}$ is set to zero in both cases. Figure 3 displays the numerical results for the concentration at various times. The dam break wave evolution washes the initial concentration distribution to the side of the tank with less initial water (upper side in the figures). Although no experimental data are available for validation in this case, it is important to note that significant differences appear. The decoupled method described by (42) generates unrealistic oscillations whilst the coupled method as in (30) produces a more appropriate and smooth solute concentration map that follows very closely the water flow motion. The flow motion has previously been calibrated by means of the experimental data [15] and, in absence of diffusion, the transport is fully dominated by the advection, that is, the flow velocity field, as Figure 4 shows for the time $t = 5\,\mathrm{s}$ after the gate removal using the numerical results obtained with the coupled methodology.

5.2. Asymmetric dam break with flat bed: diffusion techniques

The same geometry and initial conditions will be used to analyse the performance of the proposed diffusion techniques. In this case the dispersion effect is included assuming that the

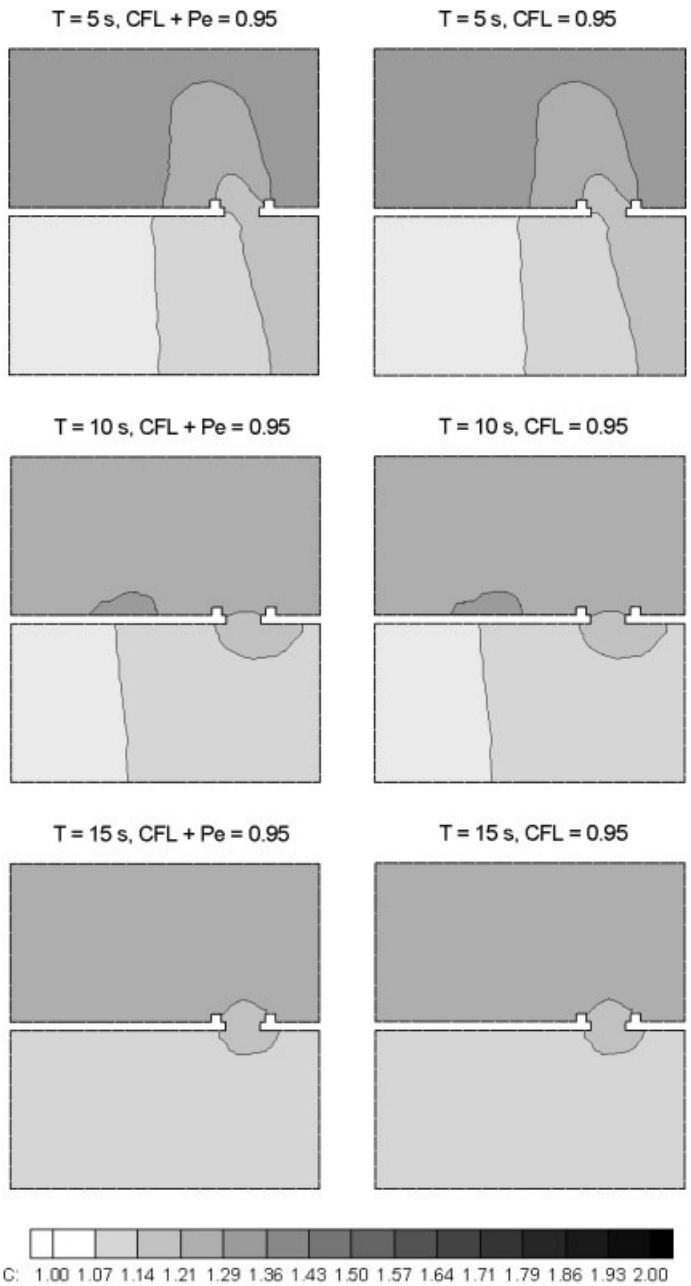

Figure 5. Isolines of concentration at times $t = 5, 10, 15$ s, computed with technique using $CFL + Pe = 0.95$ (left) and technique (right) with $CFL = 0.95$. $k_{xx} = k_{yy} = 0.1$.

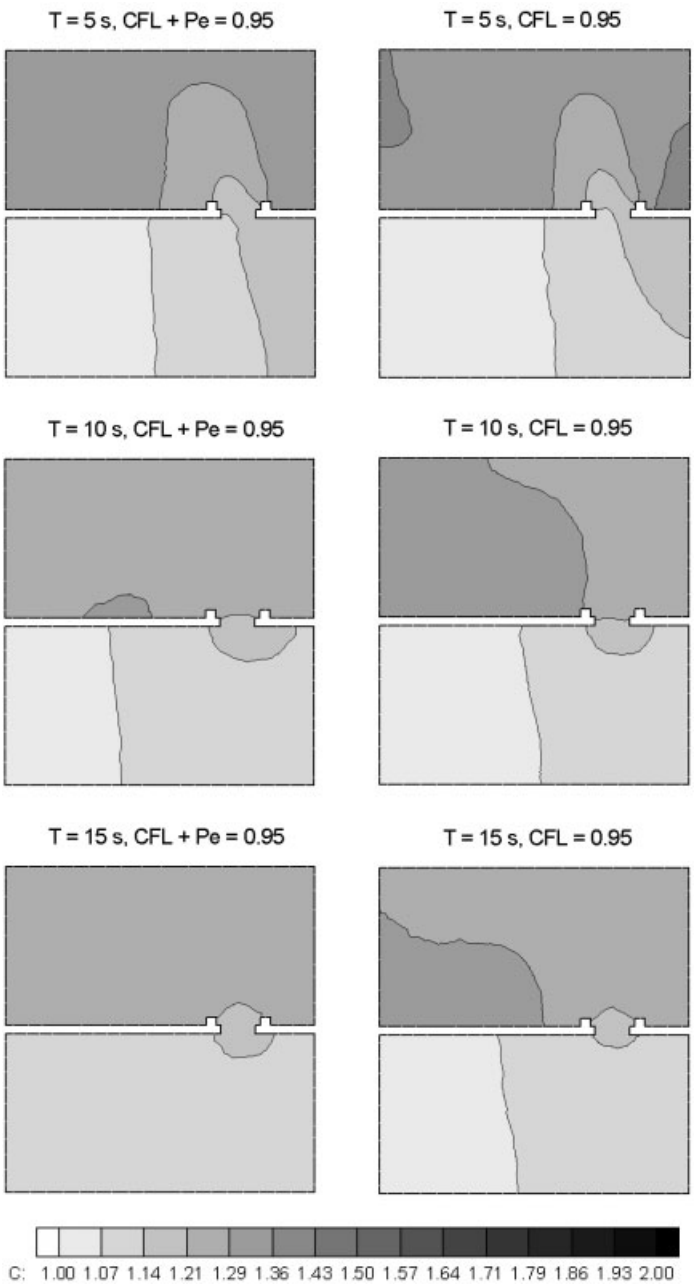

Figure 6. Isolines of concentration at times $t = 5, 10, 15$ s, computed with technique using $CFL + Pe = 0.95$ (left) and technique (right) with $CFL = 0.95$. $k_{xx} = k_{yy} = 0.1$.

Table I. Computing time and ratios. $k_{xx} = k_{yy} = 0.1$.

	Simulation time (s)	Ratio
Technique (a)	3857	5.67
Technique (b)	754	1.10
Technique (c)	680	1.00

coefficient **K**, is as

$$\mathbf{K} = \begin{pmatrix} k_{xx} & k_{xy} \\ k_{yx} & k_{yy} \end{pmatrix} = \begin{pmatrix} 0.1 & 0 \\ 0 & 0.1 \end{pmatrix}$$

which results in the special relevance of the diffusion in the whole simulation. The coupled system of equations is now used. Figure 5 displays the results when the same limit is imposed on the time step condition for techniques (a) (imposing $CFL+Pe = 0.95$) and (b) ($CFL = 0.95$) as described in earlier sections.

In Figure 6, the results when the same limit is imposed on the time step, using techniques (a) ($CFL + Pe = 0.95$) and (c) ($CFL = 0.95$) are also shown. Table I contains the computing times needed in each case, using a Pentimum IV, and the time ratios. We want to show that if technique (c) (implicit diffusion) is applied using the same time step limit as the one imposed in (a), the method leads to less diffusive solutions.

Due to the relative weight of the diffussion coefficient, there are important differences in the computing time when techniques (b) or (c) are used instead of (a). Technique (a) leads to an excessive computing time and, although technique (b) consumes almost the same computing time as technique (c), the results prove that, not only technique (c) is the less diffusive method, but it is also the most economic in CPU time. Despite being implicit, technique (c) proves to be the less diffusive option.

In the following case, the value of the coefficient **K** is decreased one order of magnitude:

$$\mathbf{K} = \begin{pmatrix} k_{xx} & k_{xy} \\ k_{yx} & k_{yy} \end{pmatrix} = \begin{pmatrix} 0.01 & 0 \\ 0 & 0.01 \end{pmatrix}$$

Hence, the resulting time step computed by means of the advection step and the one involving diffusion have approximately the same size. Hence the differences in the total computing time between the proposed techniques are negligible.

Figure 7 displays the results when the same limit is imposed on the time step condition for techniques (a) (imposing $CFL + Pe = 0.95$) and (b) ($CFL = 0.95$) as described before. The results when the same limit is imposed on the time step, using techniques (a) ($CFL+Pe = 0.95$) and (c) ($CFL = 0.95$) are shown in Figure 8. The computing time used by each technique is shown in Table II. In this case the differences in the results obtained using techniques (a), (b) or (c) are almost negligible.

As third example, the coefficient **K** is chosen as

$$\mathbf{K} = \begin{pmatrix} k_{xx} & k_{xy} \\ k_{yx} & k_{yy} \end{pmatrix} = \begin{pmatrix} 0.001 & 0 \\ 0 & 0.001 \end{pmatrix}$$

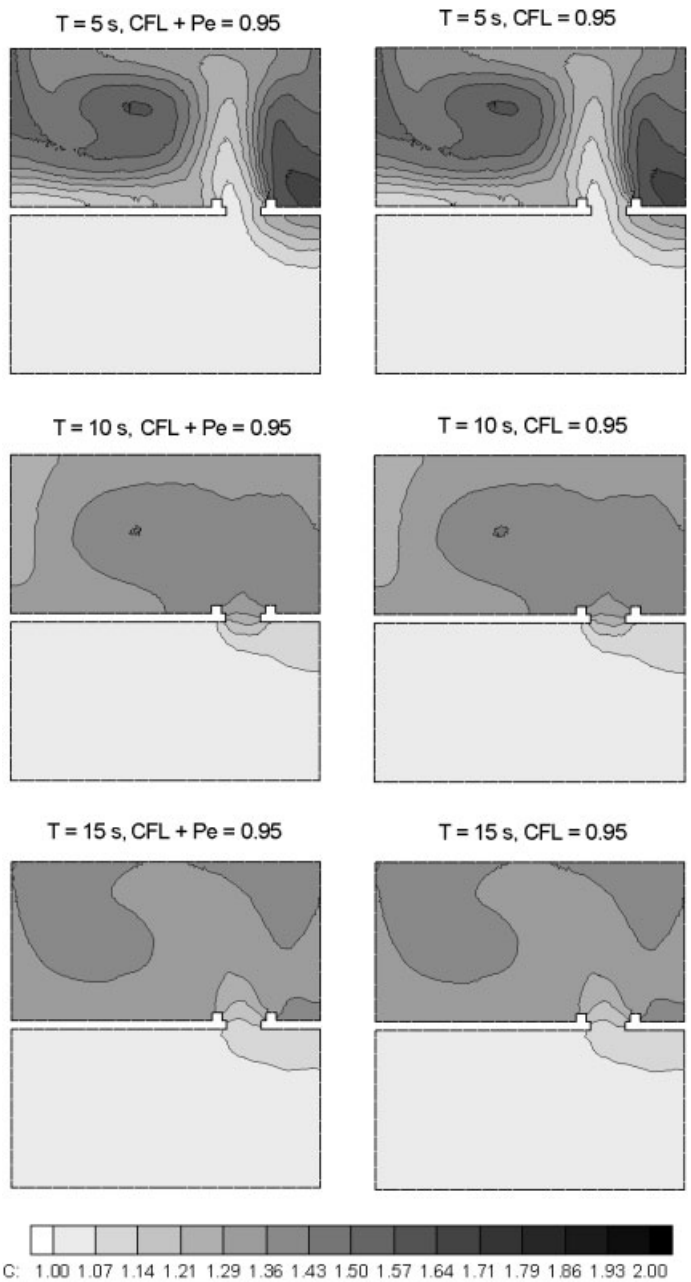

Figure 7. Isolines of concentration at times $t = 5, 10, 15$ s, computed with technique using $CFL + Pe = 0.95$ (left) and technique (right) with $CFL = 0.95$. $k_{xx} = k_{yy} = 0.01$.

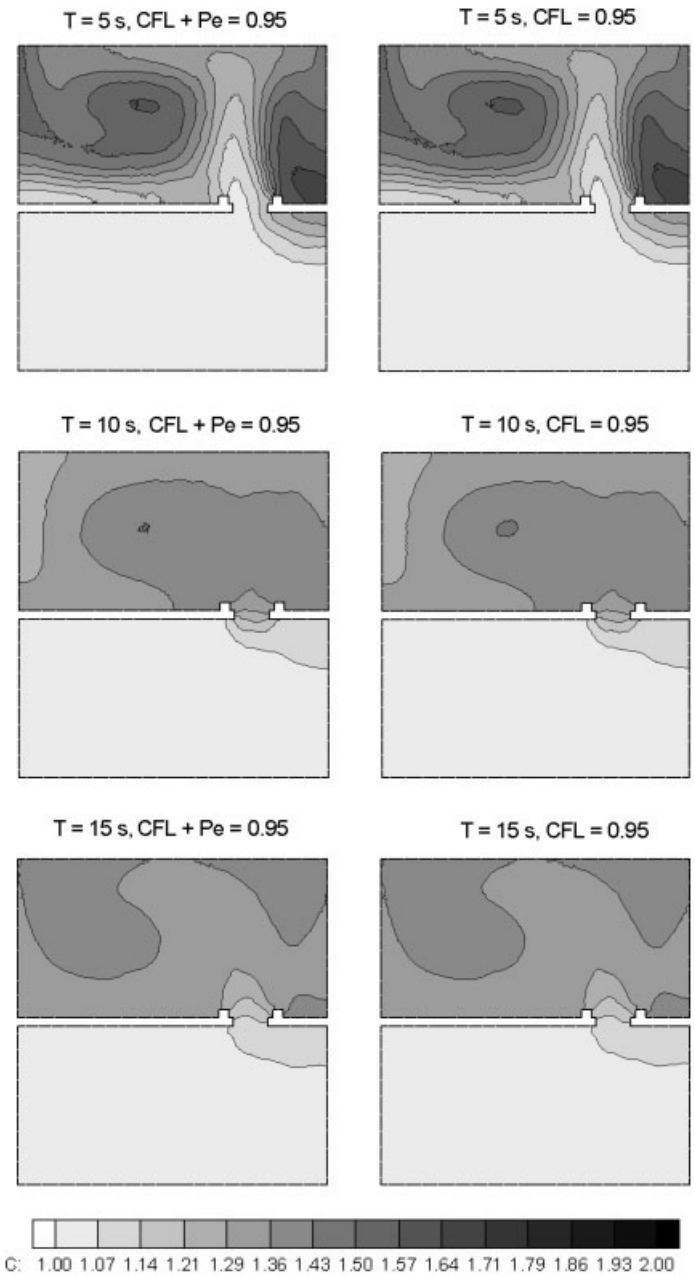

Figure 8. Isolines of concentration at times $t = 5, 10, 15$ s, computed with technique using $CFL + Pe = 0.95$ (left) and technique (right) with $CFL = 0.95$. $k_{xx} = k_{yy} = 0.01$.

Table II. Computing time and ratios. $k_{xx} = k_{yy} = 0.01$.

	Simulation time (s)	Ratio
Technique (a)	693	1.02
Technique (b)	689	1.01
Technique (c)	680	1.00

In this case the diffusion is almost negligible compared with the advection, therefore the time step size is controlled by advection. Figure 9 displays the results when the same limit is imposed on the time step condition for techniques (a) ($CFL+Pe=0.95$) and (b) ($CFL=0.95$) as described before. The results when the same limit is imposed on the time step, using techniques (a) ($CFL+Pe=0.95$) and (c) ($CFL=0.95$) are shown in Figure 10. The computing time used by each technique is shown in Table III. In this case no differences in the results are found. Figures 9 and 10 show no differences between techniques (a), (b) and (c) as expected. Also no differences are found in the computing time.

As the diffusion coefficient can vary in a wide range, we can conclude that the proposed technique (c) is the best choice, since it reduces the necessary number of time steps when the diffusion term is important, providing the less diffusive numerical results in general, and shows good agreement with the fully explicit methodology in cases of negligible diffusion.

5.3. *Steady state in presence of source terms*

The following test case is intended to study the quality of the numerical results in presence of important bed variations. Therefore, a variable bed is set within the previous example geometry. The assumed bottom elevation is given by the following function:

$$z(x,y) = -0.3\left(1 - \sin\left(\frac{d(x,y)}{2.6}2\pi\right)\right)$$

where the results are given in meters and $d=(x^2+y^2)^{1/2}$. Figure 11 displays two plots of the resulting bottom elevation.

This numerical test is oriented to evaluate the ability of the numerical approaches to preserve an initial condition of still water with uniform concentration in presence of the mentioned bed variations. This is a basic but compulsory test case for conservative methods. In this case a uniform zero velocity, water level, $h+z=0.1\,\mathrm{m}$, and a uniform value for the concentration $\phi=2$ are initially imposed over the whole domain. When the system is coupled and the source terms are discretized following the scheme proposed in (30), the system is able to keep a uniform value for the solute concentration constantly in time. But, if only the coupling of the fluxes is used as in (20) and the source terms are not carefully treated, oscillations in the solute concentration appear from the beginning. Figure 12 displays the results for both cases after one time step, and how equilibrium is already violated by not considering the complete upwind treatment of the source terms related to the bed slope.

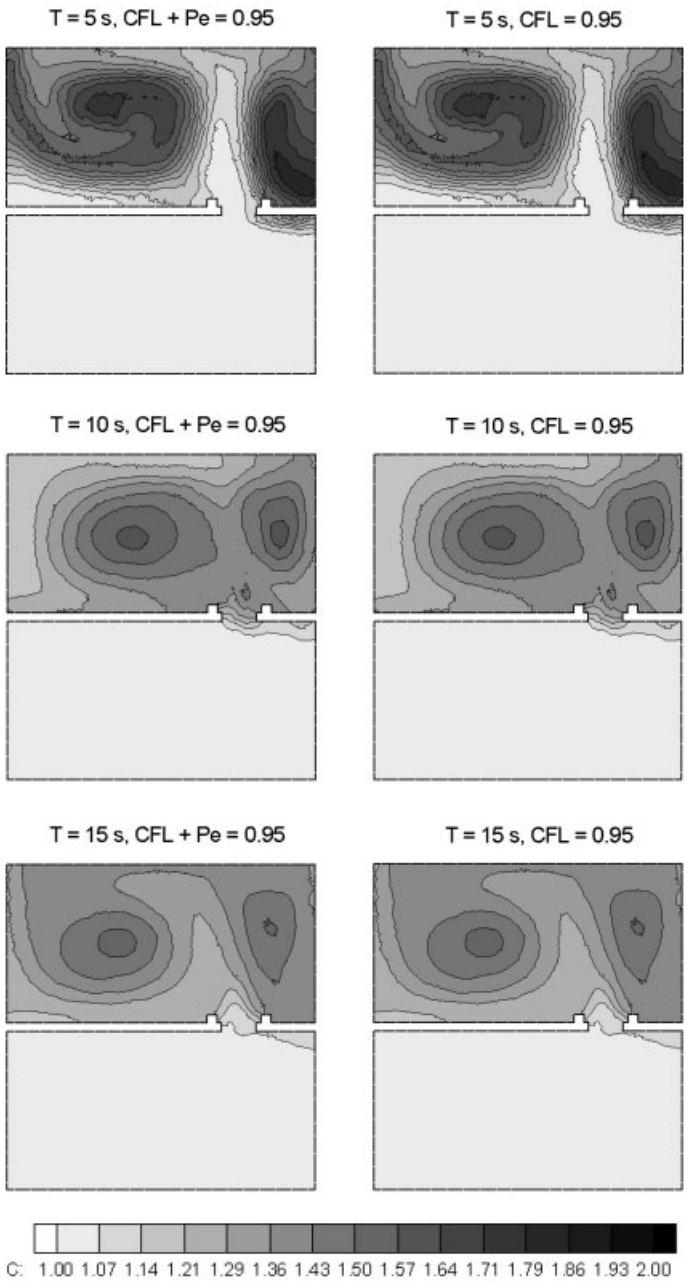

Figure 9. Isolines of concentration at times $t = 5, 10, 15$ s, computed with technique using $CFL + Pe = 0.95$ (left) and technique (right) with $CFL = 0.95$. $k_{xx} = k_{yy} = 0.001$.

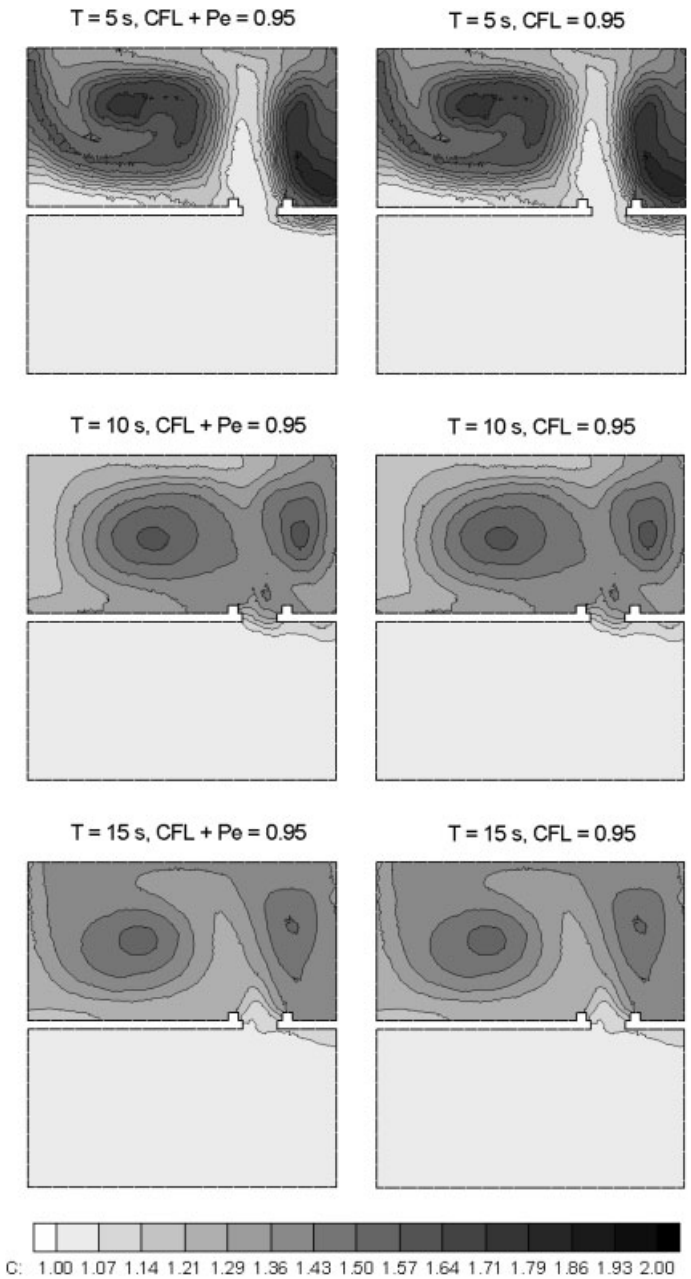

Figure 10. Isolines of concentration at times $t = 5, 10, 15$ s, computed with technique using $CFL + Pe = 0.95$ (left) and technique (right) with $CFL = 0.95$. $k_{xx} = k_{yy} = 0.001$.

Table III. Computing time and ratios. $k_{xx} = k_{yy} = 0.001$.

	Simulation time (s)	Ratio
Technique (a)	661	1.00
Technique (b)	661	1.00
Technique (c)	661	1.00

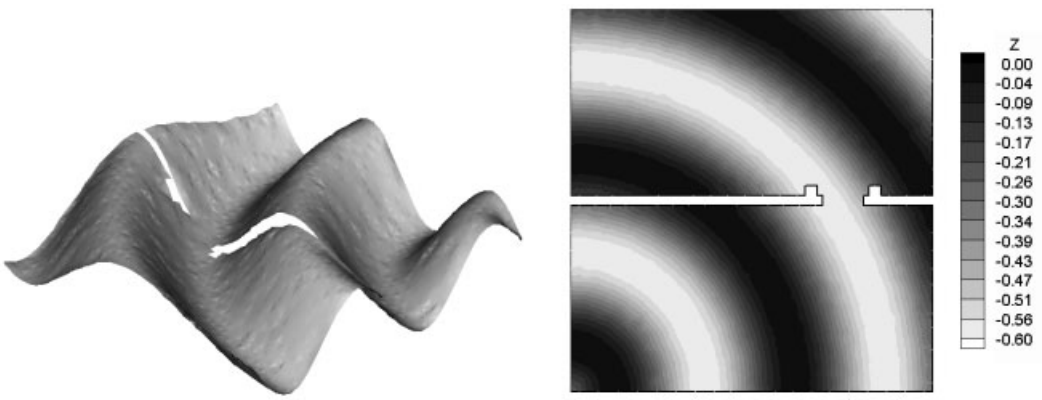

Figure 11. Bottom elevation.

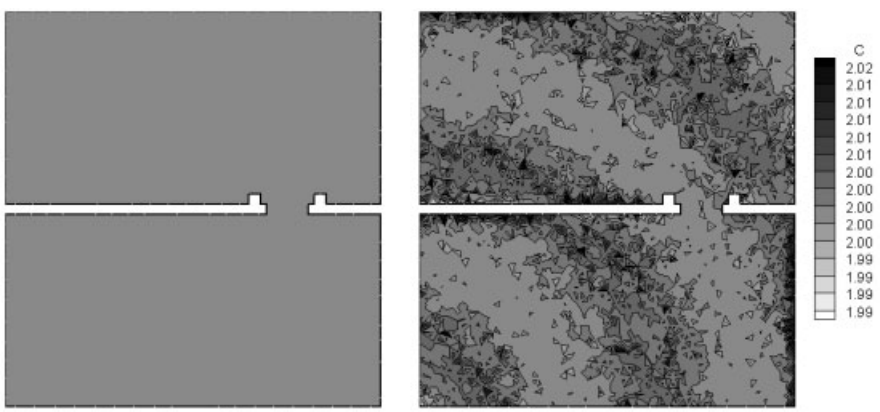

Figure 12. Solution for concentration after one time step with upwind treatment of all the source terms (left) and without including upwind treatment of all the source terms (right).

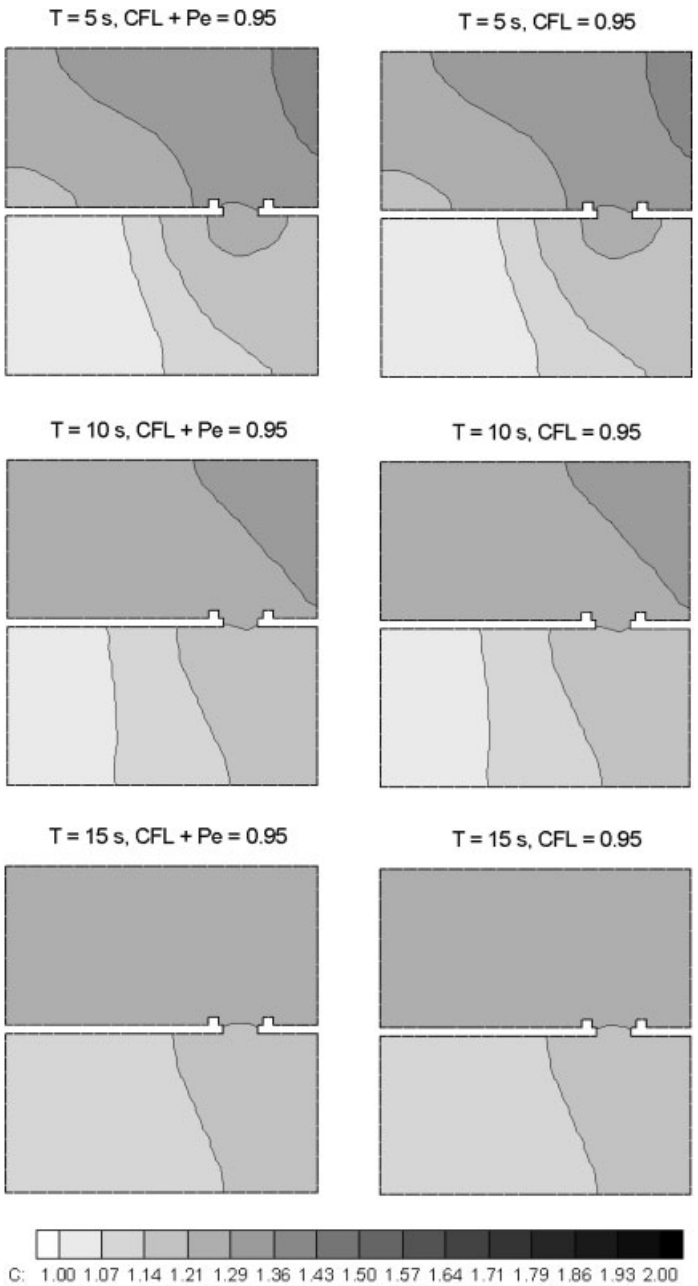

Figure 13. Isolines of concentration at times $t = 5, 10, 15$ s, computed with technique using $CFL + Pe = 0.95$ (left) and technique (right) with $CFL = 0.95$. $k_{xx} = k_{yy} = 0.1$.

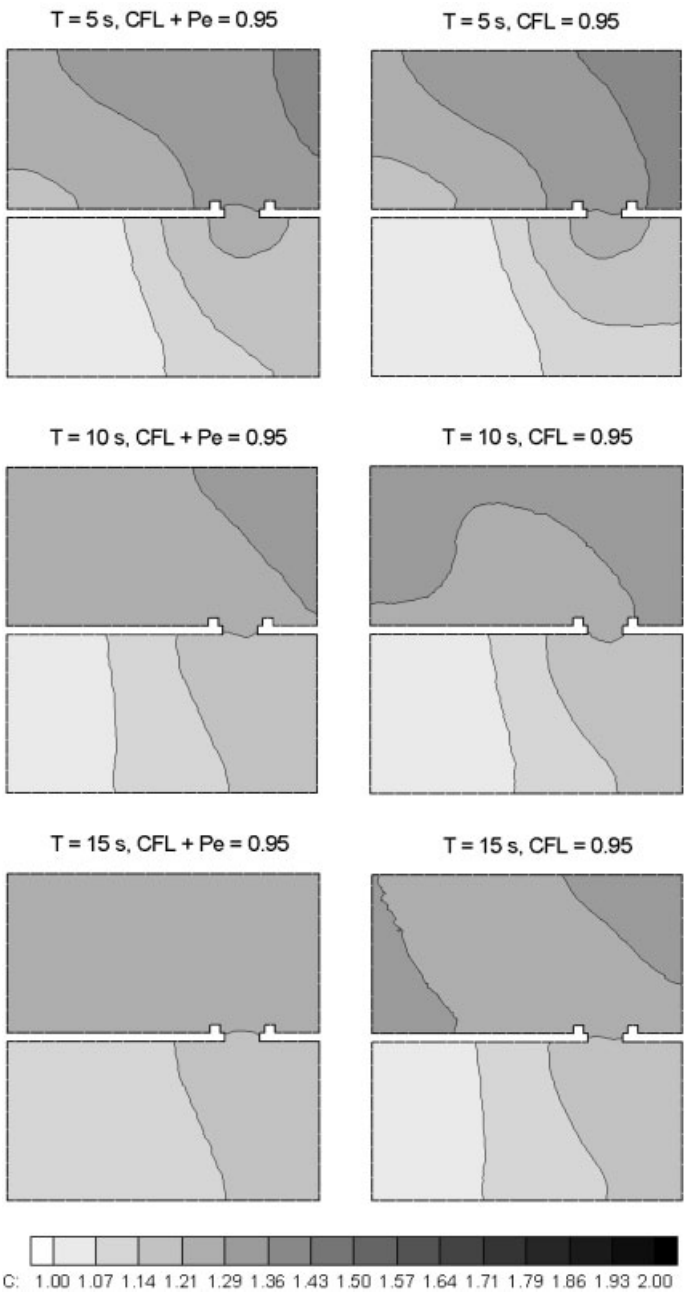

Figure 14. Isolines of concentration at times $t = 5, 10, 15$ s, computed with technique imposing $CFL + Pe = 0.95$ (left) and technique (right) with $CFL = 0.95$. $k_{xx} = k_{yy} = 0.1$.

Table IV. Computing time and ratios. $k_{xx} = k_{yy} = 0.1$. Variable bed.

	Simulation time (s)	Ratio
Technique (a)	3782	4.04
Technique (b)	859	1.00
Technique (c)	858	1.00

5.4. Asymmetric dam break with variable bed

As a final example, the complete problem of propagation including advection and diffusion over a variable bed is analyzed. The bed level variations presented in the previous section, and the initial water levels, dispersion coefficients and initial solute concentration used in Section 5.2 are put together. We shall adopt the coupled system of equations and discretize all the source terms in an upwind manner assuming these are the best options. Then we would like to compare the performances of the alternatives offered for the diffusion.

First, the value of $\mathbf{K}$ is set equal to

$$\mathbf{K} = \begin{pmatrix} k_{xx} & k_{xy} \\ k_{yx} & k_{yy} \end{pmatrix} = \begin{pmatrix} 0.1 & 0 \\ 0 & 0.1 \end{pmatrix}$$

The results for $CFL + Pe = 0.95$ using (a) and $CFL = 0.95$ using (b) are shown in Figure 13.

The results for $CFL + Pe = 0.95$ using technique (a) and $CFL = 0.95$ using technique (c) are shown in Figure 14. The computing time consumed by each technique is shown in Table IV. Again, the time step is strongly dominated by the diffusion and, as in Section 5.2, the conclusion is that technique (c) provides both the less diffusive results and the fastest simulation.

If the value of $\mathbf{K}$ is decreased ten times

$$\mathbf{K} = \begin{pmatrix} k_{xx} & k_{xy} \\ k_{yx} & k_{yy} \end{pmatrix} = \begin{pmatrix} 0.01 & 0 \\ 0 & 0.01 \end{pmatrix}$$

the results for $CFL + Pe = 0.95$ using technique (a) and $CFL = 0.95$ using (b), are shown in Figure 15. The results for $CFL + Pe = 0.95$ in (a) and CFL $= 0.95$ in (c) are shown in Figure 16. The computing times are shown in Table V. The time step size is dominated both by advection and diffusion so almost no differences are found when techniques (a), (b) or (c) are used.

When the value of $\mathbf{K}$ is reduced to

$$\mathbf{K} = \begin{pmatrix} k_{xx} & k_{xy} \\ k_{yx} & k_{yy} \end{pmatrix} = \begin{pmatrix} 0.001 & 0 \\ 0 & 0.001 \end{pmatrix}$$

the time step is controlled by the advection, and no differences are found when using techniques (a), (b) or (c). The results are displayed on Figures 17 and 18. The computing times are shown in Table VI.

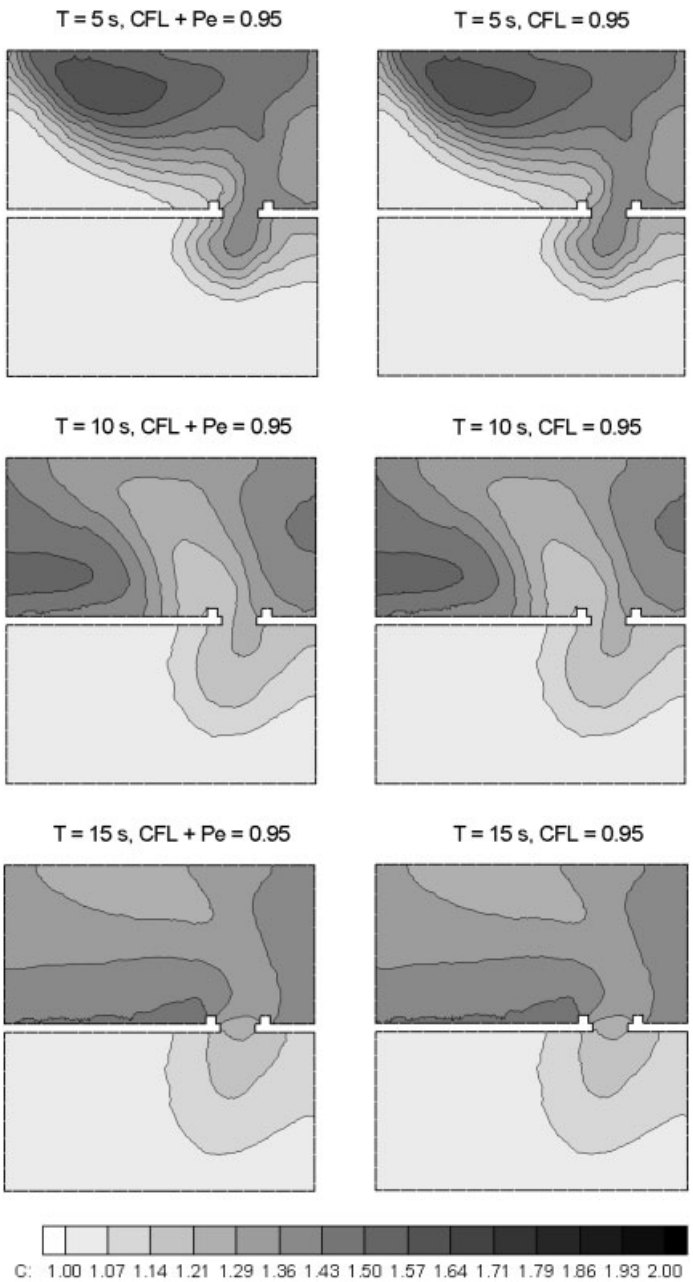

Figure 15. Isolines of concentration at times $t = 5, 10, 15$ s, computed with technique using $CFL + Pe = 0.95$ (left) and technique (right) with $CFL = 0.95$. $k_{xx} = k_{yy} = 0.01$.

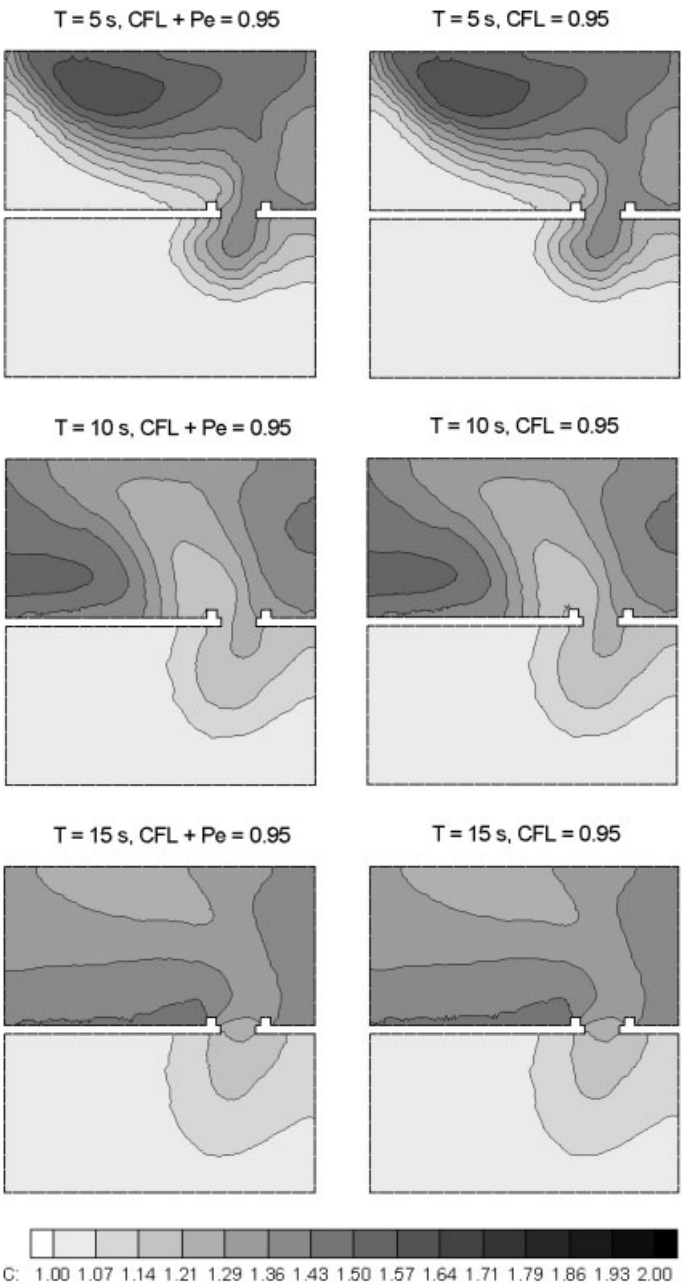

Figure 16. Isolines of concentration at times $t = 5, 10, 15$ s, computed with technique using $CFL + Pe = 0.95$ (left) and technique (right) with $CFL = 0.95$. $k_{xx} = k_{yy} = 0.01$.

Table V. Computing time and ratios. $k_{xx} = k_{yy} = 0.01$. Variable bed.

	Simulation time (s)	Ratio
Technique (a)	868	1.00
Technique (b)	865	1.00
Technique (c)	861	1.00

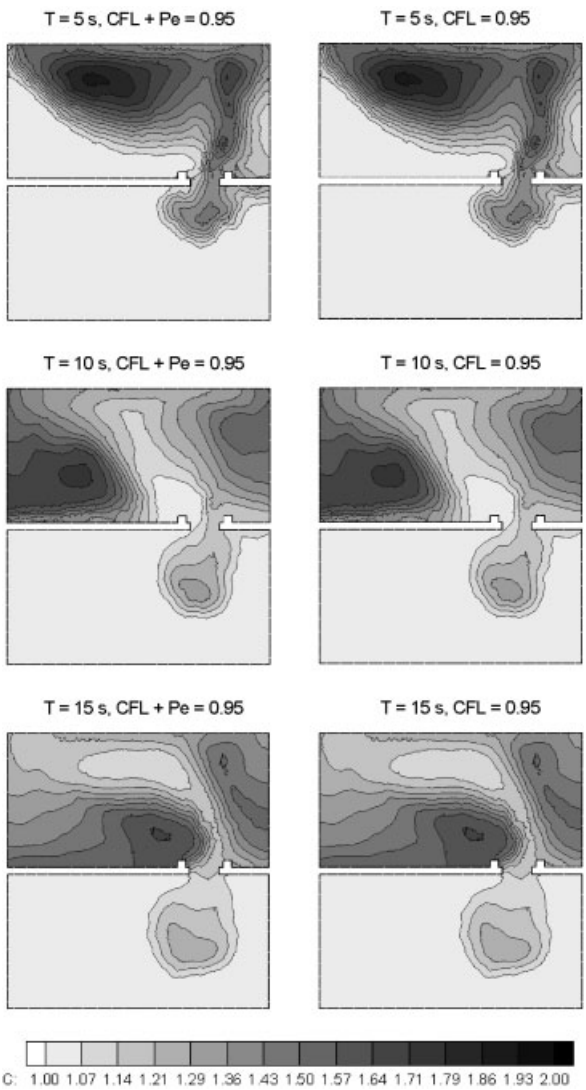

Figure 17. Isolines of concentration at times $t = 5, 10, 15$ s, computed with technique using $CFL + Pe = 0.95$ (left) and technique (right) with $CFL = 0.95$. $k_{xx} = k_{yy} = 0.001$.

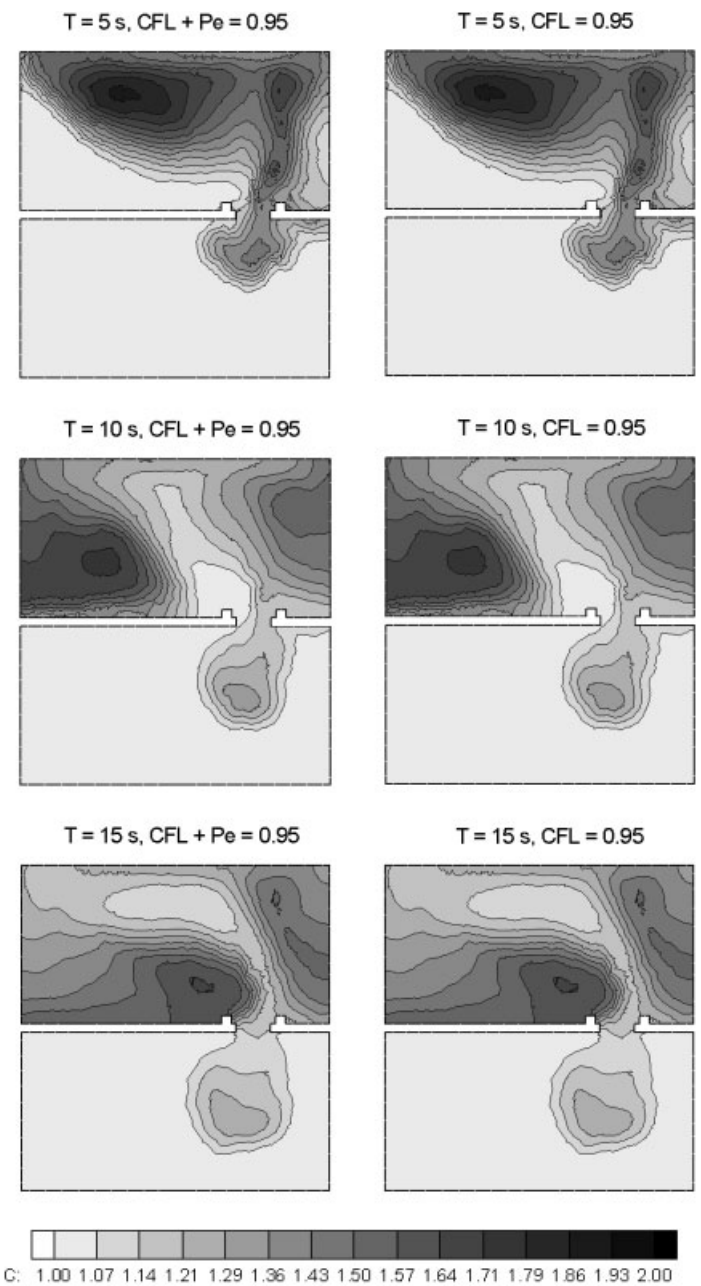

Figure 18. Isolines of concentration at times $t = 5, 10, 15$ s, computed with technique using $CFL + Pe = 0.95$ (left) and technique (right) with $CFL = 0.95$. $k_{xx} = k_{yy} = 0.001$.

Table VI. Computing time and ratios. $k_{xx} = k_{yy} = 0.001$. Variable bed.

	Simulation time (s)	Ratio
Technique (a)	852	0.99
Technique (b)	858	1.00
Technique (c)	858	1.00

6. CONCLUSIONS

A numerical model based on the conservative form of the coupled system of two-dimensional depth-averaged shallow water flow and solute transport flow has been presented. In order to build a robust and efficient model able to deal with steady and unsteady flow even in presence of discontinuities of both solute concentration and water depth, a first order upwind flux difference scheme (Roe's scheme) has been used for the solution of the frictionless non-diffusive part of the coupled system. A numerical coupling appears among the water and solute equations arising from the bottom level variation source terms. The redefinition of the Jacobian matrix not only avoids numerical oscillations when a constant concentration is present, it also reinforces the necessity of modelling bottom variations by means of an upwind approach. The model guarantees a steady state for the shallow water equations and also ensures that no solute exchange is produced when dealing with pure advection, in case of zero water velocity over a non-uniform bed level.

The numerical tests performed have demonstrated the importance of including in the same set the shallow water equations and the solute flow in a conservative form in case of pure advection in presence of water surface discontinuity over flat bed. It has also been shown that the new Jacobian matrix allows a whole treatment of the source terms leading to the correct conservation of the equilibrium state in case of variable bed.

A centred discretization has been applied to the diffusion terms and three different techniques have been considered for their time integration: fully explicit and coupled to the advective part in a single time step (a), explicit following an operator splitting algorithm (b) and implicit following an operator splitting algorithm (c). Among them, technique (c) is recommended as this cocktail leads to less diffusive solutions with less computational effort.

The conservation property in a numerical solution is not only related to the numerical scheme used but also to the discretization adopted at the boundaries. In all the examples presented, boundaries were assumed to be solid walls, hence their discretization was trivial and has not been mentioned. One of the goals to achieve as future work is the correct discretization of open boundary conditions in order to allow the inlet and outlet of solute mass in a conservative form. As a second objective, the presence of variable solute concentration in transient problems characterized by wetting/drying fronts, will be studied.

REFERENCES

1. Playán E, García-Navarro P, Zapata N. Solute transport modelling in overland flow applied to fertigation. *Journal of Irrigation and Drainage Engineering* 2000; **126**(1):33–40.
2. Weiming Wu, Dalmo A Vieira, Sam SY Wang. One-dimensional numerical model for nonuniform sediment transport under unsteady flows in channel networks. *Journal of Hydraulic Engineering* 2004; **130**(9):914–923.

3. Nakamura T, Tanaka R, Yabe T, Takizawa K. Exactly conservative semi-Lagrangian scheme for multidimensional hyperbolic equations with directional splitting technique. *Journal of Computational Physics* 2001; **174**:171–207.
4. Burguete J, García-Navarro P. Semi-Lagrangian conservative schemes versus Eulerian schemes to solve advection in river flow transport. *Proceedings of the Fifth International Conference on Hydroinformatics*, Cardiff, U.K., 2002; 181–185.
5. Brufau P, Vázquez-Cendón ME, García-Navarro P. A numerical model for flooding and drying of irregular domains. *International Journal for Numerical Methods in Fluids* 2002; **39**:247–275.
6. Brufau P, García-Navarro P, Vázquez-Cendón ME. Zero mass error using unsteady wetting–drying conditions in shallow flows over dry irregular topography. *International Journal for Numerical Methods in Fluids* 2004; **45**:1047–1082.
7. Abbot MB. *Computational Hydraulics*. Ashgate Publishing Company: New York, 1992.
8. Holly FM. Two dimensional mass dispersion in rivers. *Hydro. Paper No. 78*. Colorado State University, Fort Collins, CO.
9. Cunge JA, Holly FM, Verwey A. *Practical Aspects of Computational River Hydraulics*. Pitman Publishing Ltd.: London, 1980.
10. Hubbard ME, García-Navarro P. Flux difference splitting and the balancing of source terms and flux gradients. *Journal of Computational Physics* 2000; **165**:89–125.
11. Roe P. A basis for upwind differencing of the two dimensional unsteady Euler equations. *Numerical Methods in Fluid Dynamics II*. Oxford University Press: Oxford, 1986.
12. Leveque RJ. *Numerical Methods for Conservation Laws*. Birkhäuser: Basel, 1990.
13. Burguete J. Modelos unidimensionales de flujos de superficie libre y transporte en geometrías irregulares: Aplicación al flujo en ríos. *Ph.D. Thesis*, University of Zaragoza, 2003.
14. Karpik SR, Crockett SR. Numerical solution of transport equation for applications in environmental hydraulics and hydrology. *Journal of Hydraulic Engineering* (ASCE) 1997; **123**(5):389–401.
15. Brufau P. Simulación bidimensional de flujos hidrodinámicos transitorios en geometrías irregulares. *Ph.D. Thesis*, University of Zaragoza, 2000.

